3-D finite element analysis of flux reflection and flux concentration effects of eddy currents

3-D FINITE ELEMENT ANALYSIS OF FLUX REFLECTION AND FLUX CONCENTRATION EFFECTS OF EDDY CURRENTS

T.Yoshimoto, S.Yamada and K.Bessho

ABSTRACT

This paper deals with the flux reflection effect and the flux concentration effect of eddy currents induced in a pair of conductors with small slit between them under an a.c.-excited coil. To perform this analysis an iterative method of FEM calculation using four components is applied to the 3-D model.

By this method, the computer memory for the main system matrix can be reduced to one sixteenth, compared with the 3-D methods conventionally used. The model analyzed is a flux concentration apparatus for producing a state of high flux density through utilization of eddy currents.

ITERATIVE 3-D FEM CALCULATION

From the fact that the eddy currents generally circulate in a finite length conductor, it does not seem appropriate to use conventional 2-D FEM calculations for determining the correct distribution and effects of eddy currents.

Though several 3-D formulations have been presented, as shown in [1] and [2], one serious problem in this field is how to manage the huge system of equations resulting from four components per each node, in addition to 3-D structure. The method presented here can reduce the computer memory for the main system matrix to one sixteenth by dividing the total simultaneous equations into four groups and using an iterative process.

For a three-dimensional, quasi-stationary, eddy current diffusion problem, one fundamental equation is derived by combining Maxwell's field equations, and the other equation is derived from the fact that the divergence of the eddy current density should equal zero.
Those two equations are

$$\frac{1}{\mu}\nabla(\nabla A) - \frac{1}{\mu}\nabla^2 A = -\sigma(j\omega A + \nabla\phi) + J_s \qquad (1)$$

$$\nabla\cdot\sigma(j\omega A + \nabla\phi) = 0 \qquad (2)$$

where,
- A : three-component vector potential
- J_s: source current density
- ϕ : electric scaler potential
- μ : permeability of medium
- σ : conductivity of medium

Applying the Coulomb guage, (1) is divided into three groups of equations, so that (1) and (2) are rewritten as follows

$$-\frac{1}{\mu}\nabla^2 A_x + j\omega\sigma A_x = J_{sx} - (\sigma\nabla\phi)_x \qquad (3)$$

$$-\frac{1}{\mu}\nabla^2 A_y + j\omega\sigma A_y = J_{sy} - (\sigma\nabla\phi)_y \qquad (4)$$

$$-\frac{1}{\mu}\nabla^2 A_z + j\omega\sigma A_z = J_{sz} - (\sigma\nabla\phi)_z \qquad (5)$$

$$\nabla\cdot(\sigma j\omega(A_x\bar{u}_x + A_y\bar{u}_y + A_z\bar{u}_z) + \sigma\nabla\phi) = 0 \qquad (6)$$

where,
A_x, A_y, A_z : x-, y-, z- components of A
J_{sx}, J_{sy}, J_{sz} : x-, y-, z- components of J_s

After FEM formulated by using Galerkin's method [3], these four groups of simultaneous equations are solved by an iterative method. In the first iteration, by giving an arbitrary initial value to $\sigma\nabla\phi$, A_x, A_y, A_z in (3)$\sim$(5) are solved and those values are put into (6) for obtaining next value of $\sigma\nabla\phi$. The new value is used again to calculate (3)$\sim$(5) in the second iteration. In this way, final converged values of A_x, A_y, A_z and ϕ can be obtained. Its iteration algorithm is shown in Fig.1.

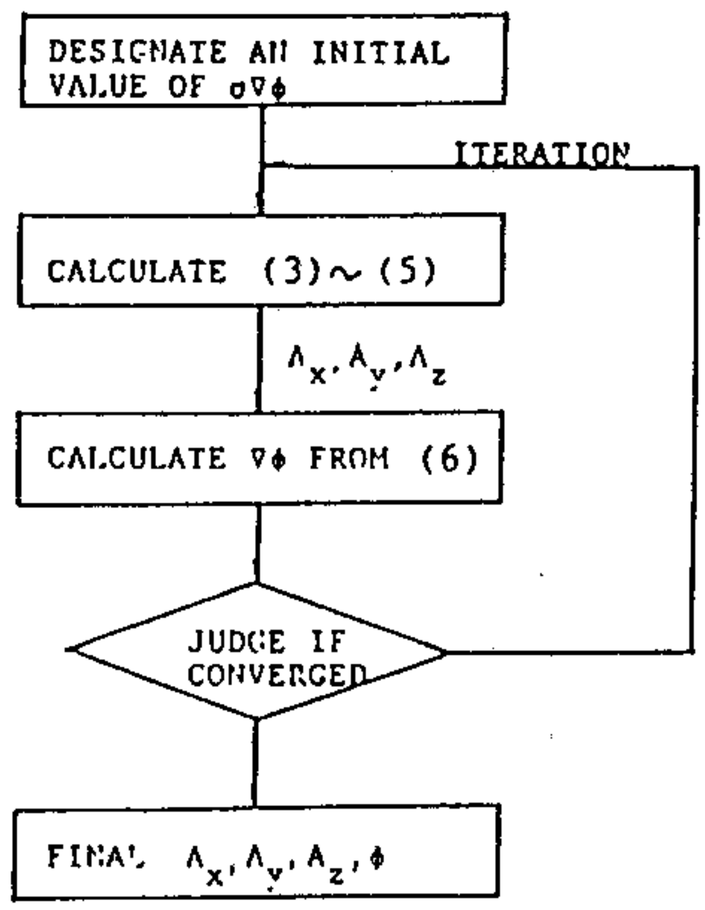

Fig.1 Flow Chart of Iteration

If the number of total nodes and the band width are assumed to be N and M, respectively per each component of A, the number of elements of the band matrix for calculating each system matrix will be N x H, while that of whole system matrix is 16 N x M. This memory saving is very effective, because the general time sharing system of the large-sized computer provides a certain limited region to an individual user.

Manuscript received May 13, 1986.

Takeshi Yoshimoto is with the Department of Electrical Engineering, Ishikawa College of Technology, Tsubata, Ishikawa, 929-03 JAPAN. Sotoshi Yamada and Kazuo Bessho are with the Electrical Energy Conversion Laboratory, Kanazawa University, Kodatsuno, Kanazawa, 920 JAPAN.

0018-9464/86/0900-0834$01.00©1986 IEEE

of the flux density versus slit-width resembles closely in its tendency the experimental data shown in Fig.5, in spite of using coarsely-divided, simplified model. We call this phenomenon flux concentration effect of eddy currents.

Meanwhile, Fig.3 (b) and Fig.4 (b) show most flux is reflected on the plate surface. This reflection effect is observed more remarkably when higher frequency is used.

Fig.6 (a) and (b) show eddy current distributions on the central plane and the top surface, respectively, when the applied frequency is 60 Hz. It must be noted that circulating eddy currents result from introducing scaler potential into (1) and (2). The scaler potential provides a voltage source for eddy currents to be continuous in a finite dimensioned conductor. It is observed that concentrated currents flowing in the edges of both conductors contribute to elevate the flux density in the air-slit. Fig.7 (a) and (b) show eddy current distributions on the central plane and the top surface, respectively, when the applied frequency is 180 Hz. We can observe skin effect clearly in this case, as expected from the fact that half the plate thickness is 5 mm against the skin depth of 4.04 mm.

CONCLUSION

A flux concentration apparatus utilizing eddy currents is analyzed by using a 3-D iterative FEM calculation. Calculations show that the flux density in the air-slit can be elevated by the eddy currents in the edges of both conductors, and the flux is reflected on the plate surface.

Our numerical method presented here enables to decrease the computer memory for 3-D system matrix to one sixteenth, compared with the methods used so far. Though this method may be applied to models with smaller division, it remains to be improved further to analyze real apparatus in general.

Hereafter, we have to examine various parameters of the model, to enhance the effect of flux concentration.

REFERENCES

[1] M.V.K.Chari et al.,"Three Dimensional Vector Potential Analysis for Machine Field Problems", IEEE Trans. Vol, MAG-18, No.2 1982, pp.436.

[2] S.J.Salon et al.,"Three Dimensional Eddy Currents using a Four Component Formulation", IEEE Trans. Vol, MAG-20, No-5 1984, pp.1992.

[3] P.P.Silvester et al.,"Finite Elements for Electrical Engineers" Cambridge University Press, London 1983.

[4] K.Bessho et al., "Asymmetrical Eddy Currents and Concentration Effect of Magnetic Flux in a High Speed Rotating Disc", IEEE Trans. Vol, MAG-21, No.5 1985, pp.1747.

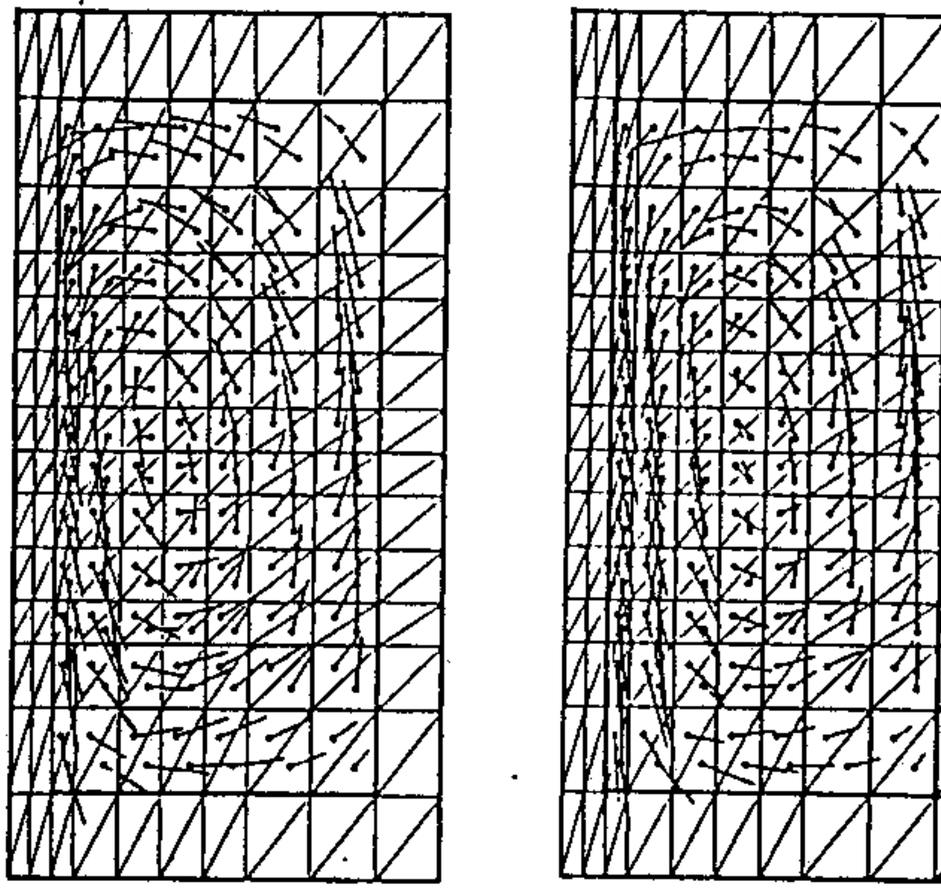

(a) at Central Plane (b) at Top Surface

Fig.6 Distribution of Eddy current Density for Applied Frequency of 60 Hz

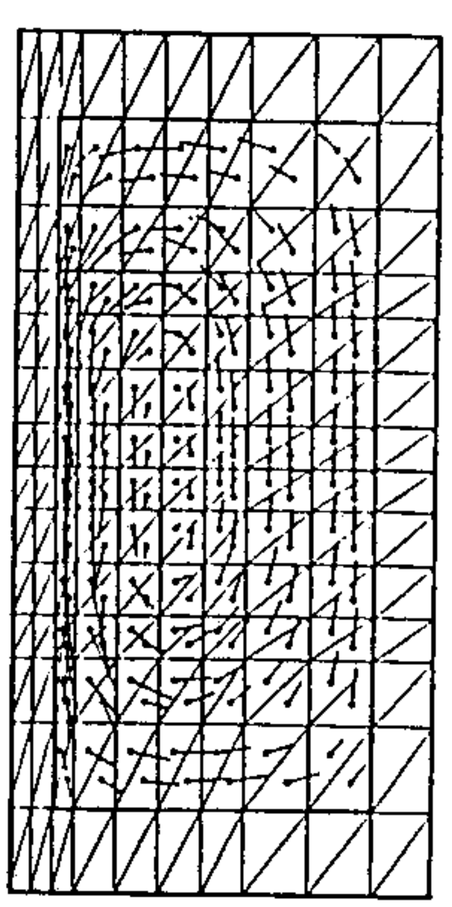

(a) at Central Plane (b) at Top Surface

Fig.7 Distribution of Eddy Current Density for Applied Frequency of 180 Hz

FLUX CONCENTRATION APPARATUS

A flux concentration apparatus utilizing eddy currents is now under investigation in Kanazawa University for the purpose of producing a state of high flux density. [4]

Its basic and simplified model shown in Fig.2 is taken to ensure the effects of eddy currents, as well as the effectiveness of the 3-D calculation method mentioned above. One eighth of the whole region is discretized and calculated, using symmetry. The a.c. current of the exciting coil is assumed to flow in sheet form. Two conductor plates are placed in parallel with a small slit. The conductor-pair is non-magnetic. Neumann condition is imposed on the outer boundary surface with zero vector potential along z- axis. Dimension of each plate is 37.5 mm (width), 80 mm (length), and 10 mm (thickness). Its conductivity is 8.62×10^7 S/m , slit width 10 mm.

Induced eddy currents in both plates show the effect of flux concentration in the air-slit and the effect of flux reflection on the top surface. As the width of the air-slit is narrowed, flux density in it is strengthened.

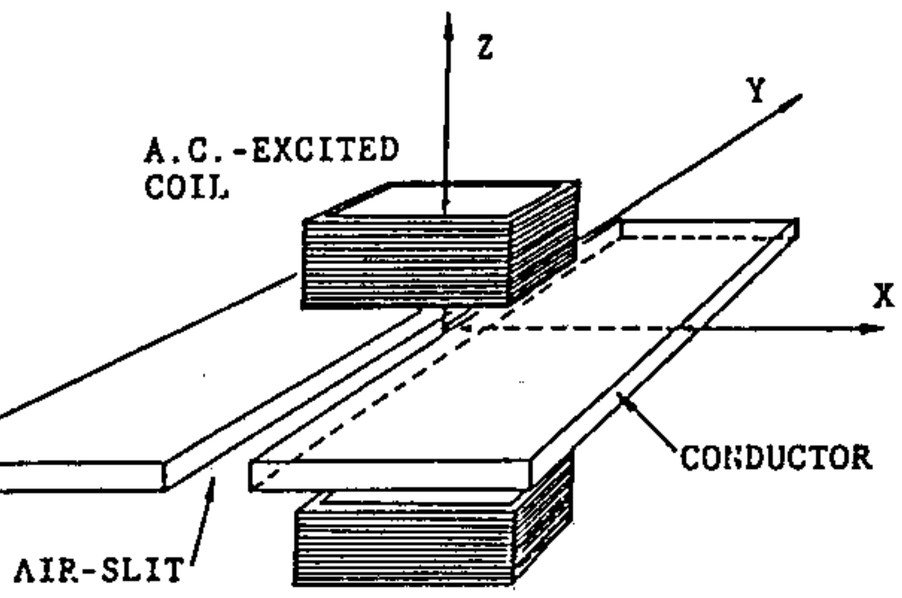

Fig.2 Simplified Model

DISTRIBUTION OF FLUX DENSITY AND EDDY CURRENTS

Calculated distributions of flux density for applied current of 60 Hz are shown in Fig.3 and Fig.4. Fig.3 and Fig.4 are for the slit-width of 10 mm and 4 mm respectively. The flux distribution along the air-slit is shown in the figure (a) for Y-Z plane, while the flux distribution across the plate is shown in the figure (b) for X-Z plane. These figures demonstrate that the flux is concentrated in the air-slit and reflected on the plate surface.

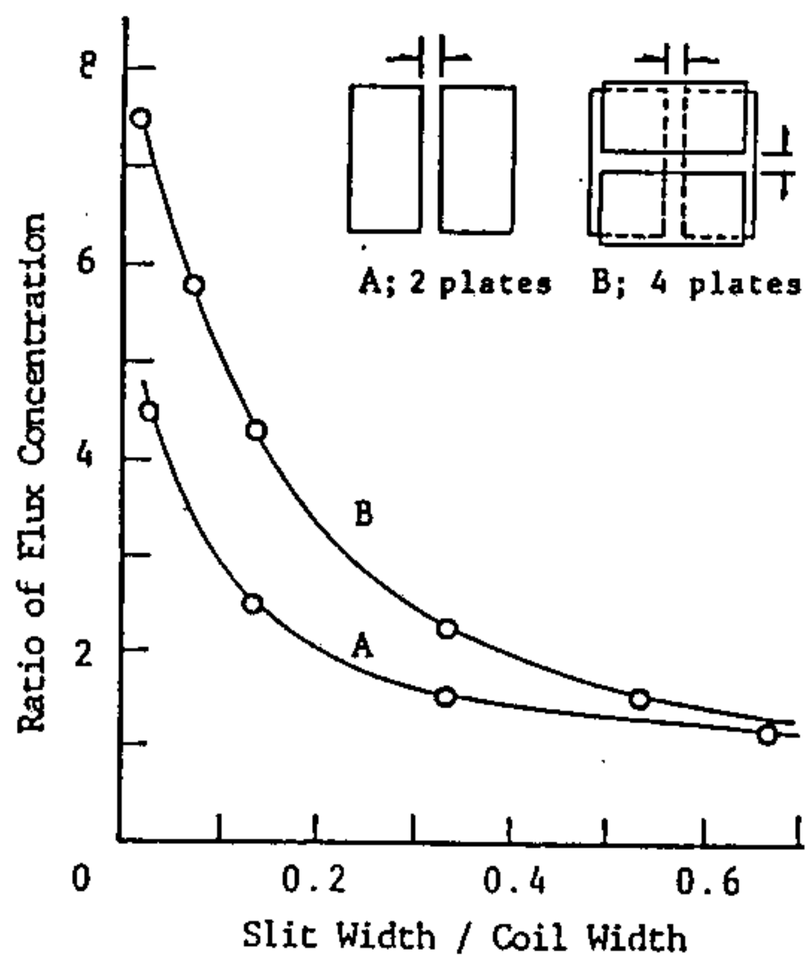

Fig.5 Ratio of Flux Concentration (Experiment)

The ratio of the maximum flux density of the slit to the average flux density of the coil increases in inverse relation to the slit-width. The characteristic

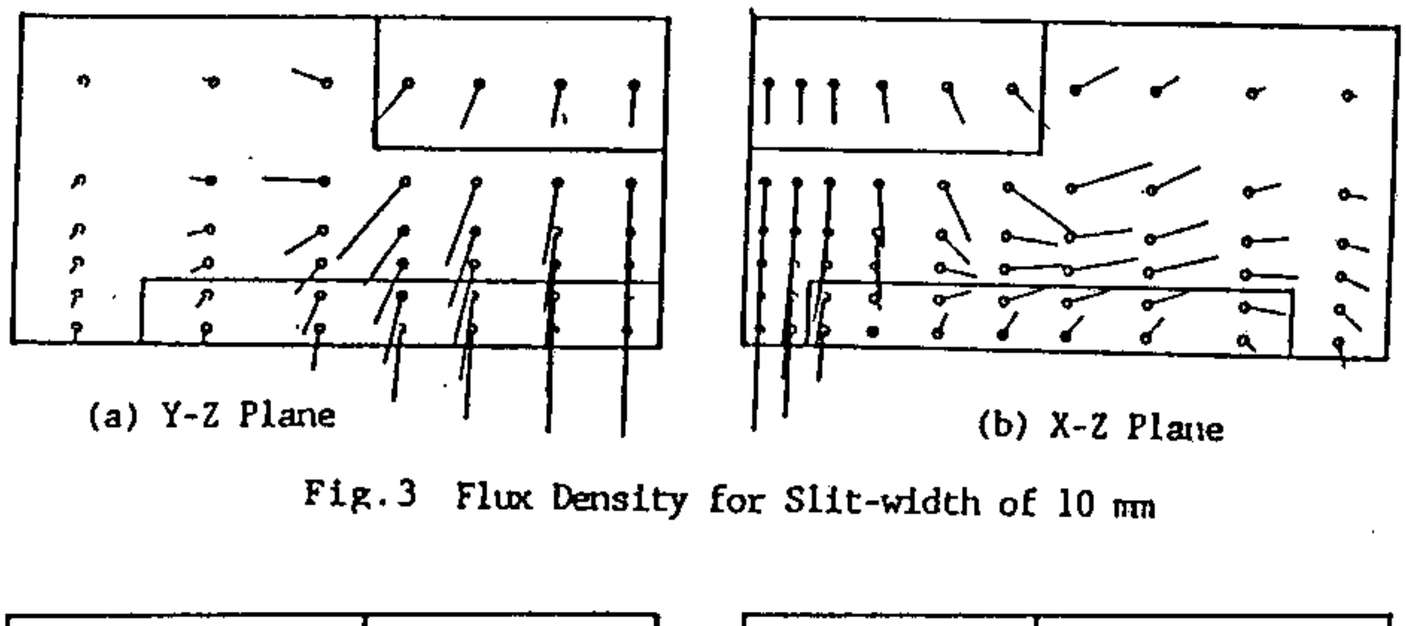

Fig.3 Flux Density for Slit-width of 10 mm

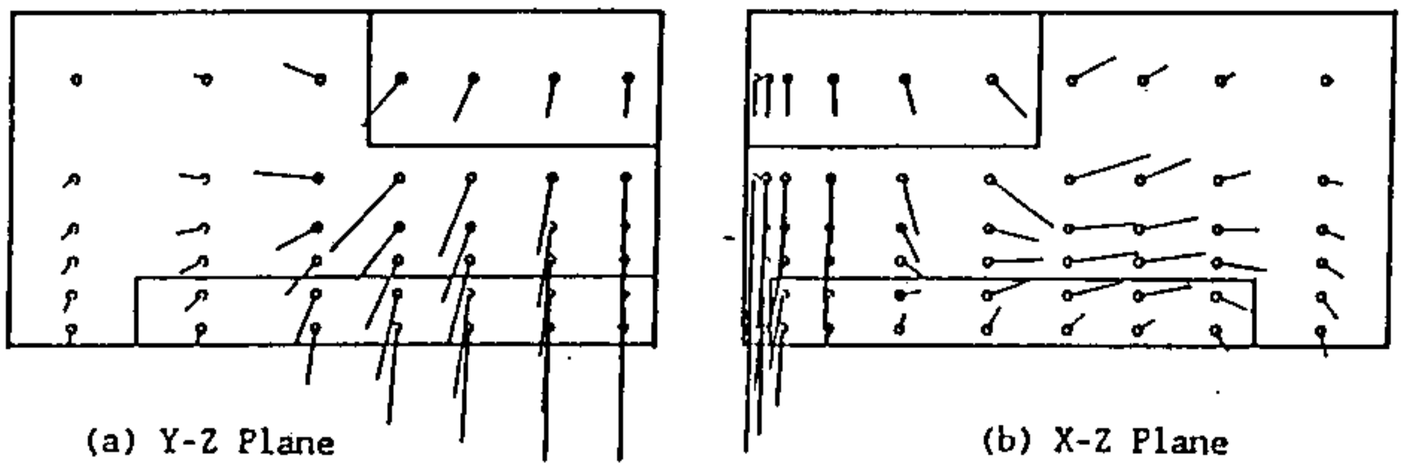

Fig.4 Flux Density for Slit-width of 4 mm